Archives of Environmental Protection
Vol. 52 no. 1 pp. 60–69

PL ISSN 2083-4772
DOI: 10.24425/aep.2026.158384

An Investigation into the Equilibrium, Isotherm, and Thermodynamic Characteristics of Mn(II) Ion Biosorption Using Pine Cones

Bashkim Thaçi*, Gentiana Hasani-Bekteshi, Albana Veseli, Arta Dylhasi,

University of Prishtina, Republic of Kosovo

*Corresponding autor`s e-mail: bashkim.thaci@uni-pr.edu

Keywords: pine cone, biosorption, thermodynamic parameters, Langmuir and Freundlich isotherms, Mn(II) ions

Abstract: It is now evident that the utilization of agricultural waste materials represents one of the most effective approaches for the remediation of heavy metal-contaminated water. In this study, Kosovo pine cones were used as a natural, low-cost biosorbent to remove Mn(II) ions from aqueous solutions. Scanning electron microscopy (SEM) and Fourier transform infrared spectroscopy (FTIR) were used to characterize the biosorbent before and after Mn(II) treatment. The observed peak shifts after Mn(II) biosorption suggest interactions between manganese ions and functional groups, particularly hydroxyl and amino groups, rather than carboxyl and carbonyl groups. The main parameters affecting the biosorption process, such as pH, biosorbent dose, initial solvent concentration, contact time, and temperature, were investigated to determine optimal conditions. The efficiency of manganese biosorption was strongly influenced by the pH of the aqueous solution, with optimal removal typically observed at a neutral pH of approximately 7. Isotherm parameters corresponding to the Langmuir and the Freundlich models were derived from the experimental data. The Langmuir isotherm model (R^2 0.997) provided the best fit to the equilibrium data, with a maximum biosorption capacity of 36.90 mg/g at 288 K. Thermodynamic parameters (ΔH^o, ΔS^o, and ΔG^o) were determined, indicating that the biosorption process is exothermic, favorable, and spontaneous. The study confirms that pine cones are an efficient biomaterial for the treatment of Mn(II)-contaminated water

Introduction

Water constitutes a fundamental prerequisite for life, serving as an essential resource for human survival and the sustenance of all living organisms. One thing is clear: without water, there is no life. As humanity advances into the third millennium, access to clean and safe drinking water has become a critical global concern, reflecting broader challenges in public health, environmental sustainability, and resource management (El Shahawy et al. 2022). High levels of heavy metals present in the environment represent a serious threat to human health and have the potential to cause substantial disturbances within ecosystems (Pholosi et al. 2020). These metals are characterized by their toxicity, mobility, and persistence in the environment, as they are non-biodegradable and can bioaccumulate in living organisms, including humans. Among them, copper, manganese, and zinc are essential trace elements involved in critical physiological processes, such as cartilage and bone formation (Deng et al. 2020). During groundwater infiltration through the Earth's crust, various inorganic compounds, including salts and metal ions such as manganese (Mn), may dissolve, potentially causing significant problems (Niksirat et al. 2019). When manganese dissolves in groundwater, it reaches the surface of this water (Pirsaheb et al. 2012). The presence of manganese in aquatic systems is often attributed to both natural processes and anthropogenic activities (Zue et al. 2016). According to guidelines established by the World Health Organization (WHO), the maximum permissible concentration of Mn(II) ions in drinking water is 0.05 mg/L (Pietrelli et al. 2019). Excessive inhalation of manganese has been associated with acute toxicity, commonly referred to as metal fume fever. Prolonged exposure can result in chronic manganese poisoning, which manifests as a range of neurological and psychological symptoms, including headaches, emotional instability, irritability, personality changes, hallucinations, hearing loss, muscular rigidity, and tremors (Deng et al. 2020).

Therefore, it is imperative to subject these wastewaters to appropriate treatment processes before their discharge into natural water bodies, such as rivers, to mitigate potential environmental and ecological harm (Lopez et al. 2019). A wide range of treatment methods has been established for the remediation of heavy metal-contaminated water, including membrane separation, chemical precipitation, ion exchange, coagulation, electrolysis, oxidative processes, and adsorption (Ali et al. 2022). However, many conventional treatment methods are associated with high operational and maintenance costs and may pose risks of secondary environmental contamination. Given the persistent and hazardous nature of heavy metal contamination, there is a critical need to advance innovative, economically viable, and highly efficient technologies for the remediation of metal-polluted environments (Dhilleswararao et al. 2019). Among the various available methods, biosorption has emerged as a particularly effective physicochemical approach for treating and purifying water and wastewater streams (Thaçi and Gashi 2019). This technique offers numerous advantages, including low operational and maintenance costs, high removal efficiencies, the absence of toxic by-products, ease of biosorbent regeneration, and the potential for multiple reuse cycles (Ali et al. 2022).

Biosorption is now widely recognized as one of the most promising and extensively applied methods for the removal of heavy metals from aqueous solutions (Ali et al. 2021; Thaçi et al. 2024). In particular, using natural biosorbents derived from locally available materials is considered especially suitable for application in developing countries, due to their affordability, accessibility, and minimal environmental footprint (Sanou and Pare 2021). Substantial research has demonstrated that agricultural waste materials represent an effective, sustainable, and environmentally friendly option for heavy metal remediation in aquatic systems (Zue et al. 2016). Among various contaminants, manganese Mn^{2+} poses a significant challenge in water treatment, particularly in regions where its concentration exceeds permissible limits. The remediation of Mn(II) remains a complex task due to technical, environmental, and operational constraints, thereby necessitating the exploration of novel biosorption strategies for effective mitigation (Ali 2017).

In recent decades, a variety of biomaterials have been investigated for their potential in manganese removal, including *Coula edulis* (Zue et al. 2016), tire residuals (Niksirat et al. 2019), *Thuja Occidentalis* leaf carbon (Dhilleswararao et al. 2019), banana peels (Ali 2017), rice husk ash (RHA) (Zhang et al. 2014), cherry kernels (Ali et al. 2022), sugarcane bagasse (Zaini et al. 2018), and chicken eggshells (Ihab and Thuraya 2021).

In this study, for the first time, Kosovo pine cones in their raw form were used as a biosorbent for the removal of Mn(II) from synthetic aqueous solutions. Fourier transform infrared spectroscopy (FTIR) and scanning electron microscopy (SEM) were used to characterize possible changes in the biomass before and after biosorption. All parameters affecting the biosorption process were investigated, and optimal values were determined. The study was conducted using a single-metal ion system and provides comprehensive insights into the feasibility of employing this natural material in wastewater remediation applications.

Material and methods

Preparation of the biosorbent and methods

The material used as a biosorbent in this research (pine cone) was obtained from the Peja region (Kosovo). This biomass was first washed several times with distilled water to remove impurities. It was then dried (80 °C for 20 h), ground, sieved, and finally the particles smaller than 0.2 mm were used for the treatment of wastewater contaminated with Mn(II) (Thaçi et al. 2023).

The FTIR spectroscopy technique (PerkinElmer Spectrum IR Version 10.6.1) was used to determine the functional groups present in the pine cones before and after treatment. The spectra were recorded in the range of 750 – 4000 cm^{-1}. The morphological structure of the pine cone surface was examined using scanning electron microscopy (SEM, ZEISS Supra 55 VP Jena). SEM imaging was carried out at an accelerating voltage of 2 kV. For analysis, the sample was mounted on an aluminum stub using carbon adhesive tape and sputter-coated with gold to enhance conductivity.

Methodology

The removal efficiency of Mn(II) ions using pine cone biosorbent was evaluated through a series of batch biosorption experiments. Stock solutions of Mn(II) were prepared at concentrations of 15, 30, 60, and 100 mg/dm^3, and biosorption trials were conducted using varying biosorbent dosages of 0.05, 0.125, 0.25, and 0.50 g. Each dosage was equilibrated with 0.050 dm^3 of the metal ion solution. To determine the optimal contact time for Mn(II) removal, experiments were performed at intervals of 5, 10, 20, 30, 60, 90, and 120 minutes. The effect of temperature was examined at 288, 298, 308, and 318 K, while the influence of pH on biosorption efficiency was evaluated over a range of pH values from 2 to 7. The pH of the solutions was adjusted using 0.1 M hydrochloric acid (HCl) or 0.1 M sodium hydroxide (NaOH) and measured with a calibrated pH meter (HANNA Instruments, HI 98130).

All biosorption experiments were performed in a thermostatically controlled shaker bath at a constant agitation speed of 200 rpm to ensure uniform mixing and temperature control. Initial experiments were conducted under the following conditions: Mn(II) concentration of 30 mg/dm^3, biosorbent dosage of 0.125 g, contact time of 30 minutes, pH 5, and temperature of 298 K. In evaluate the effect of each individual parameter on manganese biosorption, the remaining parameters were kept constant.

The concentrations of Mn(II) ions remaining in solution after biosorption were determined using flame atomic absorption spectroscopy (AAS) with a Contra AA 300 instrument (Analytik Jena). Two key performance parameters were used to assess the biosorption process: the equilibrium biosorption capacity (q_e) and the removal efficiency (%A), calculated using the following equations:

$$q_e = \frac{(C_o - C_e)V}{m} \tag{1}$$

$$\%(A) = \frac{C_o - C_e}{C_o} \cdot 100 \tag{2}$$

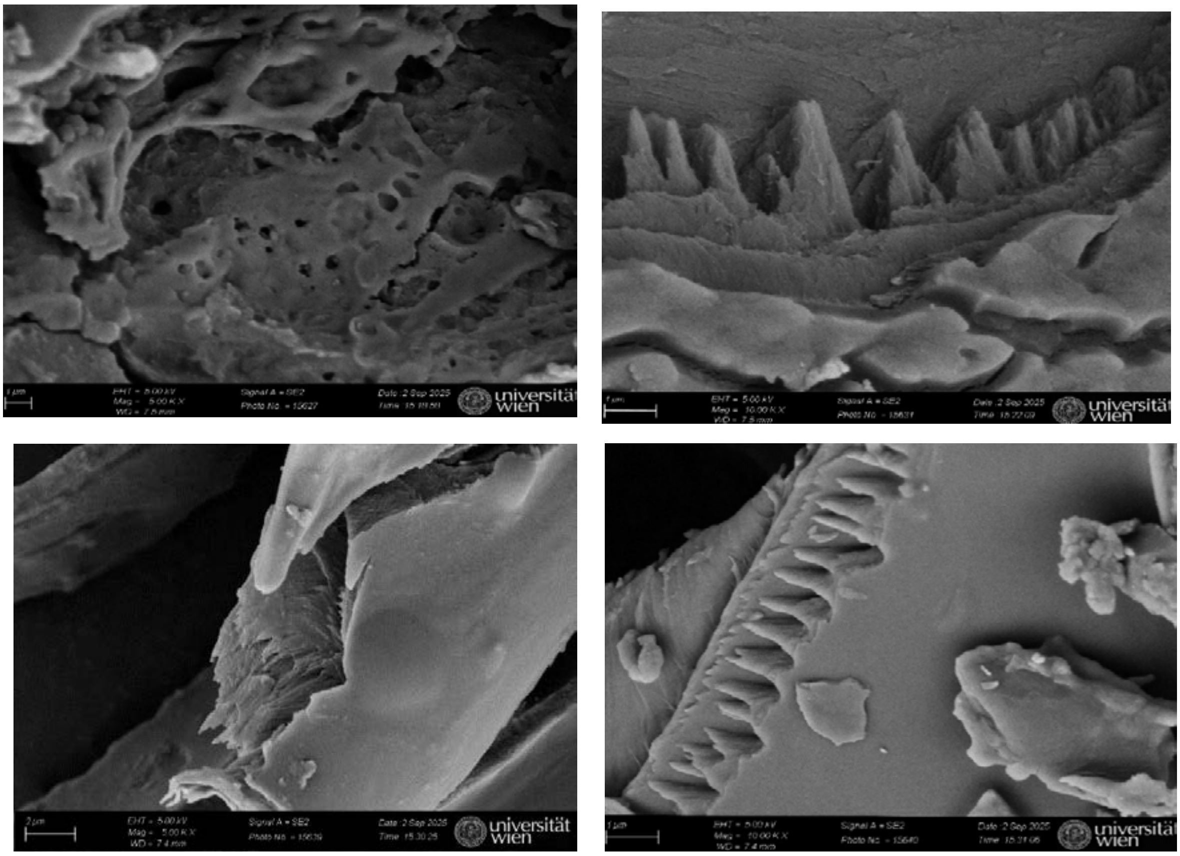

Fig 1. SEM images of pine cones as a raw biosorbent, a), b), and c), d) after biosorption of Mn(II) ions (initial conc. 30 mg/dm^3, biosorbent dosage 0.125 g, contact time 30 min, pH 5, and temperature 298 K).

where, C_0 is the initial concentration (mg/dm^3), C_e is the equilibrium concentration (mg/dm^3), V is the solution volume (dm^3), and m is the mass of the biosorbent (g).

Results and Discussion

Characterization of biosorbent

SEM method

Scanning Electron Microscopy (SEM) enables detailed visualization of surface characteristics, including pore shape, size, and distribution on the biomaterial surface. This technique is particularly useful for examining structural changes in biomass before and after the biosorption process (Asif et al. 2019). Representative SEM micrographs illustrating these features are presented in Fig. 1a and 1b for the pine cone surface before biosorption, and in Fig. 1c and 1d after the biosorption process. The SEM images presented in Fig. 1a and 1b reveal a highly porous surface morphology of the pine cone prior to Mn(II) ion biosorption. In contrast, the images in Fig. 1c and 1d, corresponding to the post-biosorption state, show a noticeably reduced surface porosity. This decrease in surface porosity can be attributed to the deposition of Mn(II) ions on the pine cone surface, which partially covers and blocks the pores.

The FTIR spectrum of pine cones

TIR spectroscopy was employed to identify the functional groups present in pine cones that may be involved in interaction with Mn(II) ions, as well as to elucidate the potential interaction mechanisms between the adsorbate and the biosorbent (Asif et al. 2019). Fig. 2 presents the FTIR spectra of the biomass before and after Mn(II) ion biosorption.

The observed shifts in wavenumbers indicate the involvement of specific functional groups in binding Mn(II) ions. A shift in the absorption band from 3304.68 cm^{-1} to 3337.85 cm^{-1} after Mn(II) biosorption suggests the participation of hydroxyl (O-H) and amino (N-H) functional groups in the binding process (Asif et al. 2019, Saranda et al. 2017). The carboxylate biosorption peak observed at 1715.85 cm^{-1} in the unloaded biomass shifted to 1733.21 cm^{-1} after Mn(II) loading.

Table 1. Separation factor R_L of pine cone for Mn(II) ions in different concentrations and temperatures.

Temp.(K)	15 mol/dm^3	30 mol/dm^3	60 mol/dm^3	100 mol/dm^3
288	0.650	0.481	0.316	0.217
298	0.669	0.503	0.336	0.233
308	0.675	0.510	0.342	0.238
318	0.698	0.535	0.365	0.256

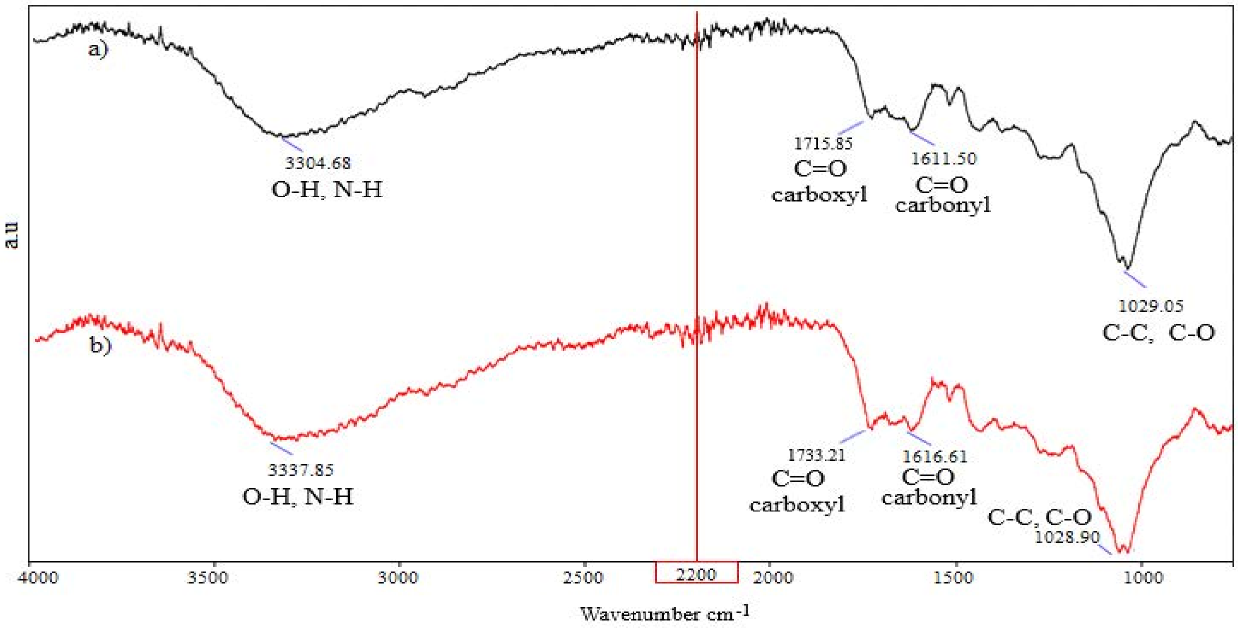

Fig 2. FTIR spectrum of pine cone before a) and b) after biosorption of Mn(II) ions (initial conc. 30 mg/dm³, biosorbent dosage 0.125 g, contact time 30 min, pH 5, and temperature 298 K).

Additionally, the carbonyl (C=O) stretching vibration band observed at 1611.50 cm⁻¹ shifted to 1616.61 cm⁻¹ following biosorption (Saranda et al. 2017).

In contrast, the vibrational bands corresponding to C–O and C–C bonds exhibited negligible shifts, changing only slightly from 1029.05 cm⁻¹ to 1028.90 cm⁻¹. Overall, the most pronounced wavenumber shifts were observed in regions associated with hydroxyl and amino groups, followed by moderate shifts in carbonyl groups. These findings indicate that hydroxyl and amino functional groups play a dominant role in the biosorption of Mn(II) ions by pine cone biomass.

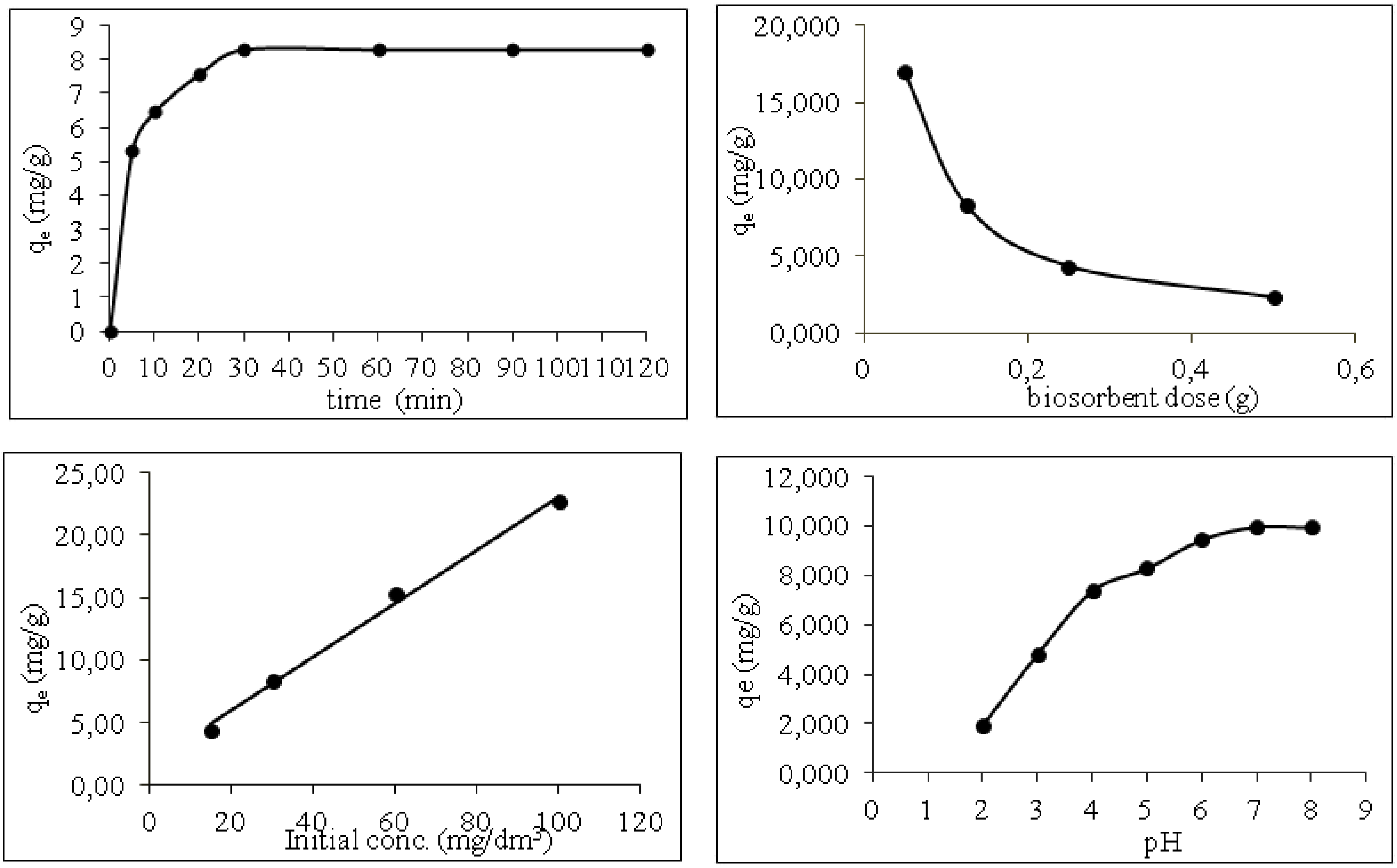

Fig 3. a) Effect of contact times, b) biosorbent dose, c) initial concentration, and d) pH on biosorption of Mn(II) ions by Pine cone.

Table 2. Langmuir and the Freundlich isotherm data for Mn(II) ions.

Langmuir isotherm parameters				Freundlich isotherm parameters		
Temp. (K)	**q_{max} (mg/g)**	**K_L (L/mg)**	**R^2**	**K_F (mg/g) $(Lmg^{-1})^{1/n}$**	**n**	**R^2**
288	36.90	0.039	0.997	1.778	1.397	0.989
298	35.91	0.033	0.998	1.683	1.425	0.995
308	35.33	0.032	0.995	1.652	1.447	0.993
318	34.84	0.029	0.997	1.545	1.449	0.995

Additional characteristics of Kosovo pine cones, including X-ray diffraction (XRD) patterns and the point of zero charge (pH_{PZC}), have been reported elsewhere (Thaçi et al. 2024).

Impact of contact time on the biosorption process

The duration of contact between the biosorbent and metal ions is a crucial operational parameter that directly influences biosorption kinetics, equilibrium attainment, and overall metal removal efficiency. Optimizing this parameter is essential for accurately assessing biosorption capacity and designing effective treatment systems (Asif et al. 2019). In this study, the effect of contact time on the biosorption of Mn(II) ions onto pine cones was investigated over a time range of 5 - 120 minutes. The corresponding results are presented in Fig. 3a.

Analysis of the biosorption data reveals that Mn(II) uptake occurs rapidly within the first five minutes, reflecting a strong affinity between the biosorbent and metal ions as well as the abundant availability of active binding sites. This rapid initial phase is followed by a markedly slower biosorption rate, indicating that the system approaches equilibrium at approximately 30 minutes (Thaçi et al. 2021). Specifically, the biosorption capacity for Mn(II) was 5.34 mg/g at 5 minutes and increased to 8.30 mg/g at 30 minutes. Consequently, extending the contact time from 5 to 30 minutes resulted in an increase of 2.96 mg/g in biosorption capacity. Beyond this period, no further enhancement in Mn(II) removal was observed with increasing contact time, which can be attributed to the rapid saturation of available biosorption sites (Saranda et al. 2017).

Impact of biosorbent dose on the biosorption process

The quantity of biosorbent employed is a critical factor influencing the removal efficiency of metal ions from solution, as it determines the biosorption capacity relative to a given biosorbate concentration and governs the extent of metal ion uptake (Mosalmani and Khayati 2025). As shown in Fig. 3b, biosorption behavior was assessed by varying the biosorbent mass (0.05, 0.125, 0.250, and 0.500 g) in 50 cm^3 of solution. The experimental results indicate that the biosorption capacity per unit mass of biosorbent decreases with increasing biosorbent dosage, particularly within the range of 0.05 - 0.25 g; this effect becomes less pronounced at higher dosages up to 0.5 g. At a biosorbent dosage of 0.05 g, the biosorption capacity reached 16.98 mg/g, whereas increasing the dosage to 0.25 g and 0.50 g resulted in a marked decline in capacity to 4.33 mg/g and 2.30 mg/g, respectively (Thaçi et al. 2025). This behavior can be attributed to increased biosorbent mass leading to particle agglomeration, which reduces the effective surface area available for biosorption (Zhang et al. 2014).

Impact of initial concentration on the biosorption process

The interaction between metal ions and the biosorbent is significantly influenced by the initial metal ion concentration (Asif et al. 2019). In this study, the effect of the initial Mn(II) ion concentration on biosorption by pine cone biomass was examined over a range of 15 - 100 mg/dm^3. The relationship between initial Mn(II) concentration and biosorption capacity is illustrated in Fig. 3c. The results show a clear increase in biosorption capacity with rising initial Mn(II) concentration within the studied range. Specifically, as the initial concentration increased from 15 to 100 mg/L, the biosorption capacity rose from 4.36 to 22.64 mg/g, with values of 4.36, 8.30, 15.34, and 22.64 mg/g recorded at initial concentrations of 15, 30, 60, and 100 mg/L, respectively. This continuous increase suggests that higher initial Mn(II) concentrations enhance the driving force for mass transfer between the solution and the biosorbent surface, thereby improving biosorption efficiency (Saranda et al. 2017).

Impact of pH on the biosorption process

Among the various factors affecting biosorption, solution pH plays a pivotal role in determining biosorption capacity and governing the interactions between metal ions and the biosorbent surface (Ali 2017). In this study, the effects of pH on the biosorption behavior of Mn(II) ions was systematically investigated over a pH range of 2 - 8, as shown in Fig. 3d. As illustrated, Mn(II) biosorption is minimal at low pH values and increases progressively with rising pH, reaching a maximum near pH 7. The biosorption capacity was found to be 1.93 mg/g at pH 2 and increased markedly to 9.99 mg/g at pH 7, with no significant variation observed between pH 7 and 8. This behavior can be attributed to competitive interactions between H^+ ions and Mn^{2+} ions for the available binding sites on the pine cone biomass at low pH values, where the high concentration of H^+ ions suppresses Mn^{2+} biosorption (Dutta et al. 2021).

At acidic pH levels, the primary functional groups on the biosorbent surface, particularly carboxyl and hydroxyl groups, become protonated, as described by the following equilibrium reaction: $R–COOH + H_3O^+ \rightarrow R–COOH_2^+ + H_2O$ (Wang et al. 2022). This protonation results in a positively charged biosorbent surface, which reduces electrostatic attraction toward cationic Mn(II) ions and consequently lowers

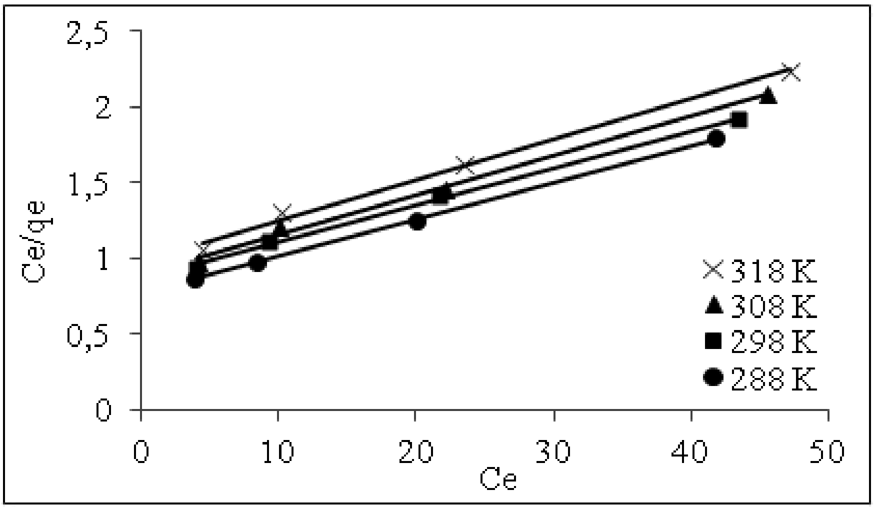

Fig 4. Langmuir isotherms for biosorption of Mn(II) ions by Pine cone.

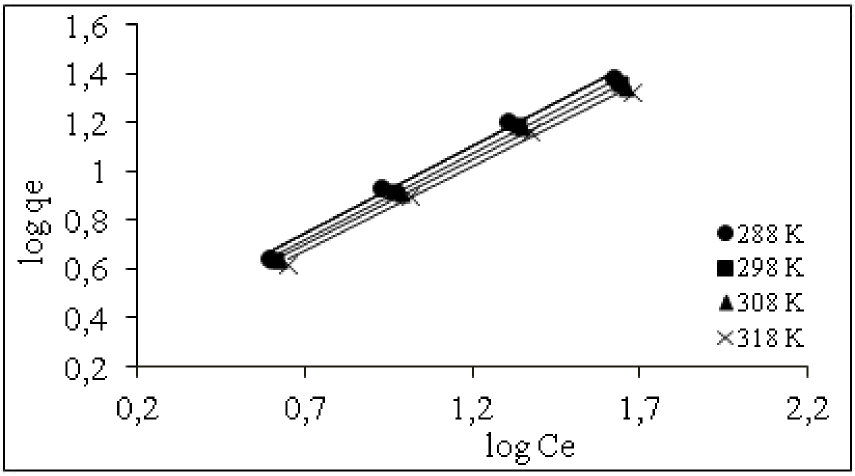

Fig 5. Freundlich isotherms for biosorption of Mn(II) ions by Pine cone.

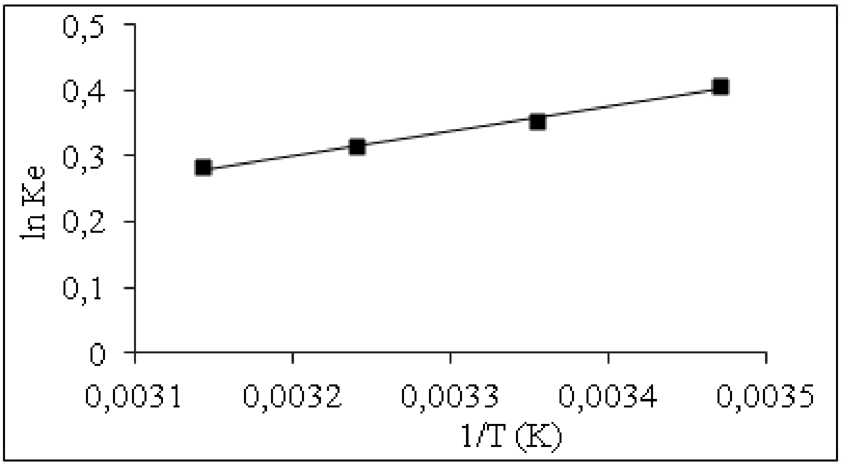

Fig 6. The plot of lnKe vs 1/T for Mn(II) ions biosorption by Pine cone.

biosorption efficiency (Pholosi et al. 2020). Conversely, as the pH increases, deprotonation of surface functional groups such as carboxyl groups (R–COOH → R–COO⁻) imparts a net negative charge to the biosorbent surface (Wang et al. 2022). This enhanced negative surface charge promotes stronger electrostatic interactions with positively charged Mn(II) ions, thereby improving biosorption performance (Pholosi et al. 2020). At pH values above 8.5, Mn(II) ions precipitate as $Mn(OH)_2$; therefore, biosorption experiments were not conducted above pH 8 to avoid interference from precipitation phenomena (Dhilleswararao et al. 2019).

Biosorbent isotherms

Biosorption isotherms play a major role in explaining the fundamental processes that regulate the interaction between biosorbents and adsorbates (Thaçi et al. 2024). They yield crucial insights into both the biosorption capacity and the kinetic behavior of the biosorption system (Mosalmani and Khayati 2025). To represent these interactions, numerous isotherm models have been formulated, each based on distinct theoretical assumptions and suited to particular environmental or experimental settings (Niksirat et al. 2019). Among the various models, the Langmuir and the Freundlich isotherms are the most widely utilized due to their strong theoretical underpinnings and demonstrated practical relevance (Dhilleswararao et al. 2019).

The Langmuir isotherm posits that biosorption occurs as a monolayer on a surface with a uniform distribution of active sites, all of which are energetically equivalent, and assumes no interaction between adsorbed molecules (Diana et al. 2020; Saranda et al. 2017). The corresponding mathematical expression for this model is given as (Diana et al. 2020):

$$\frac{C_e}{q_e} = \frac{1}{K_L q_m} + \frac{1}{q_m} C_e \tag{3}$$

where q_m denotes the maximum biosorption capacity corresponding to monolayer coverage of the adsorbent (mg/g), and K_L (L/mg) is the Langmuir constant related to the affinity of the biosorption process and biosorption energy. C_e represents the equilibrium concentration of metal ions in solution (mg/dm³), while q_e refers to the amount of Mn^{2+} ions biosorbed onto the pine cone at equilibrium (mg/g). A plot of C_e/q_e versus C_e is expected to yield a linear relationship, with a slope of $1/q_m$ and an intercept of $1/K_L q_m$. The Langmuir isotherm results for manganese ions are presented in Fig. 4.

The fundamental properties of the Langmuir model can be characterized by the separation factor (R_L) or equilibrium parameter, expressed as (Fouad et al. 2022):

$$R_L = \frac{1}{1 + K_L C_0} \tag{4}$$

For biosorption to be regarded as favorable, the separation factor R_L must satisfy the criterion $0<R_L<1$ (Zue et al. 2016). The calculated values of the separation factor are presented in Table 1.

The R_L values for pine cone, evaluated across a range of concentrations and temperatures, consistently fall within the interval of 0 to 1, thereby indicating the favorable nature of the Mn^{2+} biosorption process under the experimental conditions. As shown in Table 1, increasing the Mn^{2+} ion concentration from 15 to 100 mg/dm³ at 288 K results in a decrease in the R_L value from 0.650 to 0.217. Conversely, increasing the temperature from 288 K to 318 K at a constant concentration of 30 mg/dm³ results in an increase in R_L values, from 0.481 to 0.535. These results indicate that optimal biosorption performance is achieved at lower temperatures and higher initial Mn^{2+} ion concentrations, suggesting a more favorable interaction between the biosorbent and the adsorbate under these conditions.

According to the data presented in Table 2, the Langmuir constant (K_L) and maximum monolayer biosorption capacity (q_m) for pine cone at 288 K are 0.039 dm³/mg and 36.90 mg/g, respectively. Furthermore, as the temperature increases from 288 K to 318 K, the biosorption capacity decreases from 36.90 mg/g to 34.84 mg/g, confirming that elevated temperatures adversely affect the biosorption efficiency of Mn^{2+} ions using pine cone as biosorbent.

The Freundlich model is an empirical isotherm developed to describe biosorption on heterogeneous surfaces, allowing for multilayer formation and a variable energy of biosorption across the surface (Niksirat et al. 2019). The Freundlich biosorption isotherm can be expressed in its linearized form as:

$$\log q_e = \log K_F + \frac{1}{n} \log C_e \tag{5}$$

where K_F (mg/g)$(Lmg^{-1})^{1/n}$ is the Freundlich isotherm constant

Table 3. Data on the Mn(II) ion biosorption capacity of the various biosorbents

Biosorbents	Q_{max} (mg/g)	Ref.
Tire residuals	120.0	(Niksirat et al. 2019)
Coula edulis	15.1	(Zue et al. 2016)
Chicken eggshell	10.7	(Ihab and Thuraya 2021)
Banana peels	5.73	(Ali 2017)
Thuja Occidentalis Leaf Carbon	5.13	(Dhilleswararao et al. 2019)
Rice husk ash (RHA)	3.02	(Zhang et al. 2014)
Cherry kernel shells	2.29	(Ali et al. 2022)
Sugarcane bagasse	0.97	(Zaini et al. 2018)
Pine cone	36.90	This study

Table 4. Thermodynamic parameters of Mn(II) for the pine cone.

Temp.(K)	ΔG (kJ/mol)	ΔH (kJ/mol)	ΔS (J/Kmol)
288	-2.331	- 13.085	-37.341
298	-1.957		
308	-1.584		
318	-1.211		

related to biosorption capacity, and *1/n* is the biosorption intensity parameter, reflecting surface heterogeneity and the favorability of the biosorption process. The corresponding Freundlich isotherms are illustrated in Fig. 5, and the associated parameters are summarized in Table 2.

The biosorption of manganese ions onto the biosorbent shows a stronger correlation with the Langmuir isotherm model (R^2 0.997) than with the Freundlich model (R^2 0.989) at 288K, supporting the assumption of monolayer biosorption on a uniform surface. Furthermore, the calculated Freundlich biosorption intensity parameter ($1<n<10$) confirms the favorable nature of the biosorption process, as values within this range are indicative of efficient and beneficial biosorption behavior (Zue et al. 2016).

Table 3 presents a comparative evaluation of the biosorption capacities of various biosorbents for Mn^{2+} ions. The results reveal that, among the biosorbents investigated, only one material (tire residuals) exhibits a Mn(II) ion biosorption capacity greater than that of pine cone. This observation highlights the superior biosorption efficiency of pine cone as a biosorbent for the removal of Mn(II) ions from aqueous solutions.

Thermodynamic Studies

Temperature plays a crucial role in assessing the interactions between biosorbent materials and metal ions, as it can markedly affect the biosorption process by either enhancing or hindering the uptake of metal ions (Niksirat et al. 2019). This study systematically examined the influence of temperature on the biosorption of Mn^{2+} ions over the temperature range of 288–318 K. To elucidate the mechanisms and spontaneity of the biosorption process, the thermodynamic parameters (ΔG°, ΔH°, ΔS°) were calculated. Notably, ΔG° is an essential parameter, as it indicates the feasibility of a chemical process (Saranda et al. 2017). A negative ΔG° value signifies a spontaneous process, whereas a positive value indicates non-spontaneity. The thermodynamic parameters were calculated using the following equation:

$$\Delta G^\circ = -RT\ln K_e \qquad (6)$$

$$K_e = \frac{(C_O - C_e)}{C_e} \qquad (7)$$

$$\Delta G^\circ = \Delta H^\circ - T\Delta S^\circ \qquad (8)$$

$$\ln K_e = \frac{\Delta H^\circ}{RT} + \frac{\Delta S^\circ}{R} \qquad (9)$$

The thermodynamic parameters were obtained by applying the Van't Hoff equation. In this equation, ΔG° denotes the Gibbs free energy change, R is universal gas constant, T represents the absolute temperature, ΔH° is the standard enthalpy change, ΔS° is standard entropy change, and K_e is the equilibrium constant. A linear correlation was observed in the Van't Hoff plot of $\ln K_e$ versus 1/T, from which the slope and intercept were used to calculate ΔH° and ΔS°, respectively, as demonstrated in the Fig. 6.

As shown in Table 4, temperature exerts a negative influence on the biosorption of Mn(II) ions onto pine cone biomass, indicating that the biosorption process becomes less favorable at elevated temperatures. Higher temperatures promote the desorption of manganese ions from the pine cone surface, thereby reducing the overall sorption capacity. The negative values of ΔG° confirm that the biosorption of Mn(II) ions is spontaneous and thermodynamically favorable (Mosalmani and Khayati 2025). However, the decrease in magnitude of ΔG° with increasing temperature suggests a reduced feasibility of the biosorption process at higher temperatures. Moreover, the negative value of standard enthalpy change ($\Delta H^\circ = -13.085$ kJ/mol) indicates that the biosorption of Mn(II) ions on pine cones is exothermic in nature (Lakshmipathy and Saranda 2015). The negative standard entropy change ($\Delta S^\circ = -37.341$ J/molK) suggests a decrease in randomness at the solid–solution interface during biosorption, reflecting a reduction in the degrees of freedom of the biosorbed species (Azza et al. 2013).

Conclusions

This study was conducted to investigate the biosorption properties of pine cones for the removal of manganese ions from aqueous solutions. FTIR spectra obtained before and after biosorption showed shifts in wavenumbers, particularly those associated with hydroxyl and amine functional groups, confirming their involvement in the binding of Mn^{2+} ions. SEM micrographs clearly reveal distinct morphological changes on the biomass surface following biosorption, indicating a reduction in surface porosity due to the incorporation of Mn(II) ions. The biosorption capacity increased with contact time and reached equilibrium after 30 minutes. Under optimal experimental conditions, a maximum Mn^{2+} removal capacity of 36.90 mg/g was achieved using pine cones. The Langmuir isotherm model provided a better fit than the Freundlich model, confirming that the biosorption process follows a monolayer biosorption mechanism. The negative values of the standard enthalpy change and standard entropy change of manganese were 13.085 kJ/mol and 37.341 J/molK, respectively. Gibbs free energy was negative at all temperatures, showing that biosorption is spontaneous. These findings demonstrate that pine cone biomass exhibits significant potential as a sustainable, efficient, and low-cost biosorbent for the removal of Mn(II) ions from aqueous environments. The favorable biosorption performance of pine cones can be attributed to their porous structure and the abundance of active surface functional groups.

Conflict of Interest

The authors declare no conflict of interest.

Acknowledgement

We acknowledge support by "X and the Faculty Center for Nano Structure Research" at theUniversity of Vienna.

References:

Ali, A. (2017). Removal of Mn(II) from water using chemically modified banana peels as efficient adsorbent. *Environmental Nanotechnology, Monitoring and Management,* 7, pp. 57-63, 2017, DOI:10.1016/j.enmm.2016.12.004

Ali, K., Yehya, K., Maher, A. & Khaled, A. (2022). Removal of Cr(III), Mn(II), Fe(III), Ni(II), Cu(II), Zn(II), and Pb(II) from Water Solutions Using Activated Carbon Based on Cherry Kernel Shell Powder. *Iranian Journal of Chemistry and Chemical Engineering,* 41, 11, pp: 3687-3705. DOI:10.30492/IJCCE.2021.523406.4539

Ali, Y. A. E. H., N'diaye, A. D., Fahmi, D., Kankou, M. & Stitou, M. (2021). Adsorption of Congo red from aqueous solution using Typha australis leaves as a low-cost adsorbent. *Journal of Environmental Treatment and Technology,* 9, 2, 534–539. DOI: 10.47277/JETT/9(2)539

Asif, M. K., Umar, F., Muhammad, M. A. & Muhammad, S. (2019). Biosorption of Cd(II) ions from its aqueous solutions using powdered branches of Trifolium Resupinatum: Equilibrium and kinetics. *Green Chemistry Letters and Reviews.* 12, 3, pp. 217–224. DOI:10.1080/17518253.2019.1625976.

Azza, M., Abdel, A., Nabila, S. A., Hany, H., Abdel, G. & Ali, R. K. (2013). Biosorption of Cadmium and Lead from aqueous solution by fresh water Alga Anabaena Sphaerica Biomass, *Journal of Advances Research,* 4, 4, pp. 367–374. DOI:10.1016/j.jare.2012.07.004

Deng, H., Li, Q., Huang, M., Li, A., Zhang, J., Li, Y., Li, Sh., Kang, C., & Mo, W. (2020). Removal of Zn(II), Mn(II) and Cu(II) by adsorption onto banana stalk biochar: adsorption process and mechanisms, *Water Science & Technology*, 82, 12, pp. 2962-2974. DOI:10.2166/wst.2020.543

Dhilleswararao, V., Subbarao, M.V. & Muralikrishna, M.P.S. (2019). Removal of Manganese (II) from Aqueous Solution by Chemically Activated Thuja Occidentalis Leaves Carbon (CATLC) as an Adsorbent: Adsorption Equilibrium and Kinetic Studies. *Physical Chemistry Research,* 7, 1, pp.11-26. DOI: 10.22036/pcr.2018.149256.1539

Diana, Ch. G., Noemi, O. L., Ana, M. F. M. & Jorge, Ch. S. (2020). Adsorption behavior of Pb(II), Cd(II), and Zn(II) onto Agave Bagasse, characterization, and mechanism. *ACS Omega,* 5, 7, pp. 3302−3314. DOI:10.1021/acsomega.9b03385.

Dutta, D., Borah, J. P. & Puzari, A. (2021). Adsorption of Mn^{2+} from Aqueous Solution Using Manganese Oxide-Coated Hollow Polymethylmethacrylate Microspheres (MHPM). *Adsorption Science & Technology,* 2021, ID 5597299, pp. 1-10. DOI:10.1155/2021/5597299.

El Shahawy, A., Mubarak, M. F., El Shafie, M. & Hesham, M. A. (2022). Adsorption of Mn(II) ions from wastewater using an AgNPs/GO/chitosan nanocomposite material. *RSC Advances*, 12, pp. 29385–29398. DOI:10.1039/d2ra04693h.

Fouad, M. B., Abdelghani, B., Aicha, Ch., Belgacem, T. & Djelloul, A. (2022). Comparative study of Pb(II) adsorptions from water on used cardboard and powdered activated carbon. *Membrane and Water Treatment,* 13, 2, pp. 73 – 83. DOI:10.12989/mwt.2022.13.2.073

Ihab, A A. & Thuraya, M A. (2021). Removal of manganese (Mn^{2+}) from aqueous solution by low-cost adsorbents and study the adsorption thermodynamics and kinetics. *Journal of Physics: Conference Series,* 1773, 1, pp. 1-13. DOI:10.1088/1742-6596/1773/1/012038

Lakshmipathy, R. & Sarada, N. C. (2015). Metal ion free watermelon (Citrullus lanatus) rind as adsorbent for the removal of lead and copper ions from aqueous solution. *Desalination and Water Treatment,* 57, 33, pp. 1-11. DOI:10.1080/19443994.2015.1072064.

Lopez, J., Reig, M., Gibert, O. & Cortina, J. L. (2019). Increasing sustainability on the metallurgical industry by integration of membrane nanofiltration processes: acid recovery. *Separation and Purification Technology*, 226, pp. 267–277. DOI:10.1016/j.seppur.2019.05.100

Mosalmani, A. & Khayati, G. (2025). Thermodynamic and Kinetic Study of Diazinon Adsorption by Rice Bran from Aqueous Solution. *Iranian Journal of Chemistry and Chemical Engineering*, 44, 5, pp. 1327-1337. DOI:10.30492/IJCCE.2025.2045660.6887

Niksirat, M., Sadeghi, R. & Esmaili, J. (2019). Removal of Mn from aqueous solutions by activated carbon obtained from tire residuals. *SN Applied Sciences*, 1, 782, DOI: 10.1007/s42452-019-0797-5.

Pholosi, A., Naidoo, E. B. & Ofomaja, A. E. (2020). Intraparticle diffusion of Cr(VI) through biomass and magnetite coated biomass: A comparative kinetic and diffusion study. *South African Journal of Chemical Engineering*, 32, pp. 39–55, DOI: 10.1016/j.sajce.2020.01.005.

Pietrelli, L., Ippolito, N. M., Ferro, S., Dovi, V. G. & Vocciante, M. (2019). Removal of Mn and As from drinking water by red mud and pyrolusite. *Journal of Environmental Management*, 237, pp. 526–533. DOI: 10.1016/j.jenvman.2019.02.093

Pirsaheb, M., Dargahi, A. & Farrokhi, M. (2012). The efficiency of iron and manganese removal from groundwater using tower aeration. *Zahedan Journal of Research in Medical Science*, 14, 117.

Sanou, Y. & Pare, S. (2021). Comparative Study of Adsorption Capacity of two mixed materials for arsenic remediation. *Journal of Environmental Treatment and Technology*, 9, 3, pp. 57 – 63. DOI: 10.47277/JETT/9(3)565

Saranda, B., Prasad, M. K., Kumar, K. K. & Murthy, Ch. V. R. (2017). Biosorption of Cd^{2+} by Green Plant Biomass, Araucaria Heterophylla: Characterization, Kinetic, isotherm and thermodynamic studies. *Applied Water Science,* 7, 9, pp. 3483–3496. DOI:10.1007/s13201-017-0618-1.

Thaçi, B S. & Gashi, S. (2019). Reverse Osmosis Removal of Heavy Metals from Wastewater Effluents Using Biowaste Materials Pretreatment. *Polish Journal of Environmental Studies,* 28, 1, pp. 337-341. DOI: 10.15244/pjoes/81268.

Thaçi, B. S., Daci-Ajavazi, M., Daci, N. & Gashi, S. (2023). Removal of Zinc (II) ions by Wheat Bran and Waste Coffee as low-cost biosorbents. *Iranian Journal of Chemistry and Chemical Engineering*, 42, 1, pp. 111-122. DOI:10.30492/IJCCE.2022.541673.4995.

Thaçi, B. S., Gashi, S., Daci, N. & Daci-Ajvazi, M. (2021). Hybrid processes evaluation of Pb(II) removal from wastewater effluents. *Polish Journal of Environmental Studies,* 30, 4, pp. 3261-3267. DOI:10.15244/pjoes/130457.

Thaçi, B. S., Gashi, S.T., Daci, N.M., Podvorica, F. I. & Sopaj, F. (2024). A versatile study of single and binary removals of Pb(II) and Cd(II) ions from aqueous solutions using pine cone as biosorbent. *Desalination and Water Treatment,* 319, pp. 1 - 10, 100465. DOI:10.1016/j.dwt.2024.100465.

Thaçi, B., Gashi, S., Podvorica, F., Sopaj, F., Hasani, G., Veseli, A. & Prado-Roller, A. (2025). Study of lignite as the raw material for adsorption of Pb(II) and Cd(II) ions from aqueous solution. *Archives of Environmental Protection*, 51, 3, pp. 31 - 39. DOI: 10.24425/aep.2025.156007

Wang, Q., Wang, Y., Yang, Z., Han, W., Yuan, L. & Zhang, L. (2022). Efficient removal of Pb(II) and Cd(II) from aqueous solutions by mango seed biosorbent. *Chemical Engineering Journal Advances*, 11, 2022, pp. 1-10. DOI:10.1016/j.ceja.2022.100295

Zaini, H. & Abubakar, S. S. (2018). Adsorption Kinetics of Manganese (II) in wastewater of Chemical laboratory with Column Method using Sugarcane Bagasse as Adsorbent. *Journal of Physics: Conference Series*, 953, 1, pp. 1 - 9. DOI:10.1088/1742-6596/953/1/012022

Zhang, Y., Zhao, J., Jiang, Zh., Shan, D. & Lu, Yan. (2014). Biosorption of Fe(II) and Mn(II) Ions from Aqueous Solution by Rice Husk Ash. *Biomed Research International*, 2014, ID 973095, pp. 1 – 10. DOI:10.1155/2014/973095

Zue, M. M. & Makani, Eba, T. F. (2016). Removal of Mn (II) from Aqueous Solutions by Activated Carbons Prepared from *Coula edulis* Nut Shell. *Journal of Environmental Science and Technology*, 9, 2, pp. 226-237. DOI: 10.3923/jest.2016.226.237